Supporting Information

Boron-Nitrogen Framework Substituted Anthracene as "Hot Exciton" Fluorophores for Efficient Sky-Blue Narrowband Emissive OLEDs with Full-Width at Half-Maximum below 30 nm

Jieying Lin,[a] Ruicheng Wang,[a] Dehua Hu,*[ab] Ziquan Lu,[a] Yueyan Zhang,[a] Zecong Ye,*[ab] Yanping Huo,[abc] Shaomin Ji,*[ab]

[a] School of Chemical Engineering and Light Industry, Guangdong University of Technology, 510006, Guangzhou, P. R. China.

[b] Guangdong Provincial Laboratory of Chemistry and Fine Chemical Engineering Jieyang Center, Jieyang 515200, China.

[c] Analytical & Testing Center, Guangdong University of Technology, 510006 Guangzhou, P. R. China.

E-mail: dehuahu@gdut.edu.cn, smji@gdut.edu.cn, yezecong@gdut.edu.cn

General procedures

The reagents and solvents for the synthesis and measurements were used as received without any further purification. ^{1}H, ^{13}C measurements were recorded with y a Bruker AVANCE III HD-400 NMR spectrometer. High-resolution mass spectra (HRMS) were recorded by atmospheric pressure chemical ionization (APCI) method with a Thermo Scientific Q Exactive instrument. A STA409PC Thermogravimetric Analyzer and a NETZSCH thermal analyzer (DSC 204 F1) were used to measure the decomposition temperature (5% weight loss, T_d) and glass transition temperature (T_g), respectively. The tests were performed at a heating rate of 10 °C min^{-1} under an N_2 atmosphere. Single crystals were grown in CH_2Cl_2/n-Hexane mixtures, and the crystallographic data were collected at 100 K on a Rigaku Oxford Diffraction Supernova Dual Source (Cu at Zero) diffractometer equipped with an AtlasS2 CCD using Cu Kα radiation. Data reduction was carried out with the diffractometer's software. The structures were solved by direct methods using Olex2 software, and the non-hydrogen atoms were located from the trial structure and then refined anisotropically with SHELXL-2014 using a full-matrix least squares procedure based on F^2. The weighted R factor, wR and goodness-of-fit S values were obtained based on F^2. The

hydrogen atom positions were fixed geometrically at the calculated distances and allowed to ride on their parent atoms. All UV-vis absorption spectra were measured on a Shimadzu UV-2700 spectrophotometer. PL spectra were recorded on an Edinburgh FLS980 spectrometer. PL quantum yields were measured with an integrating sphere. Cyclic voltammetry (CV) was recorded in acetonitrile of tetra-*n*-butylammoniumhexafluorophosphate (Bu_4NPF_6) (0.1 M) with a scan rate of 100 mV s^{-1} in an Autolab PGSTAT302N electrochemical workstation using a three-electrode cell (Ag/AgCl reference electrode, Pt wire counter electrode, and glassy carbon working electrode). Fc/Fc^+ (0.18 eV against Ag/AgCl) was used as an internal standard for calibrating the reference electrode. The energy level of HOMO and LUMO were calculated according to the equation of [HOMO = -(E_{onset} + 4.8) eV] and [LUMO = (HOMO +E_g) eV], where E_{onset} is the onset oxidation potentials, and E_g is the optical bandgap obtained from the absorption onset. The ground state geometries were optimized using the density function theory (DFT) method with B3LYP functional at the basis set level of 6-31 G, and the ΔE_{ST} values were calculated by time-dependent DFT (TD-DFT) method at the B3LYP/6-31G level. NTOs analysis was conducted in Multiwfn 3.8 code.[1] Based on the optimized S_0 molecular geometries, the spin-orbit coupling matrix elements (SOCEMs) between two first singlet and triplet excited states were calculated in B3LYP/6-31 G (d,p) level using Orca 4.1.2 package.

OLED fabrication and measurement

The glass substrates precoated with a 90-nm layer of indium tin oxide (ITO) with a sheet resistance of 15~20 Ω per square were successively cleaned in an ultrasonic bath of acetone, isopropanol, detergent, and deionized water, respectively, taking 10 minutes for each step. Then, the substrates were dried in a 70 °C oven. Before the fabrication processes, to improve the hole injection ability of ITO, the substrates were treated with O_2 plasma for 10 minutes. The vacuum-deposited OLEDs were fabricated under a pressure of $< 5 \times 10^{-4}$ Pa in the Suzhou Fangsheng OMV-FS380 vacuum deposition system. Organic materials, LiF and Al were deposited at rates of 1~2 A s^{-1}, 0.1 A s^{-1}, and 5 A s^{-1}, respectively. The effective emitting area of the devices was 9 mm^2, determined by the overlap between the anode and cathode. The luminance-voltage-current density characteristics, external quantum efficiency, and EL spectra were obtained via a PhotoResearch PR670 spectroradiometer, with a Keithley 2400 Source Meter. All the characterizations were conducted at room temperature in ambient conditions without any encapsulation, as soon as the devices were fabricated.

Experimental procedures

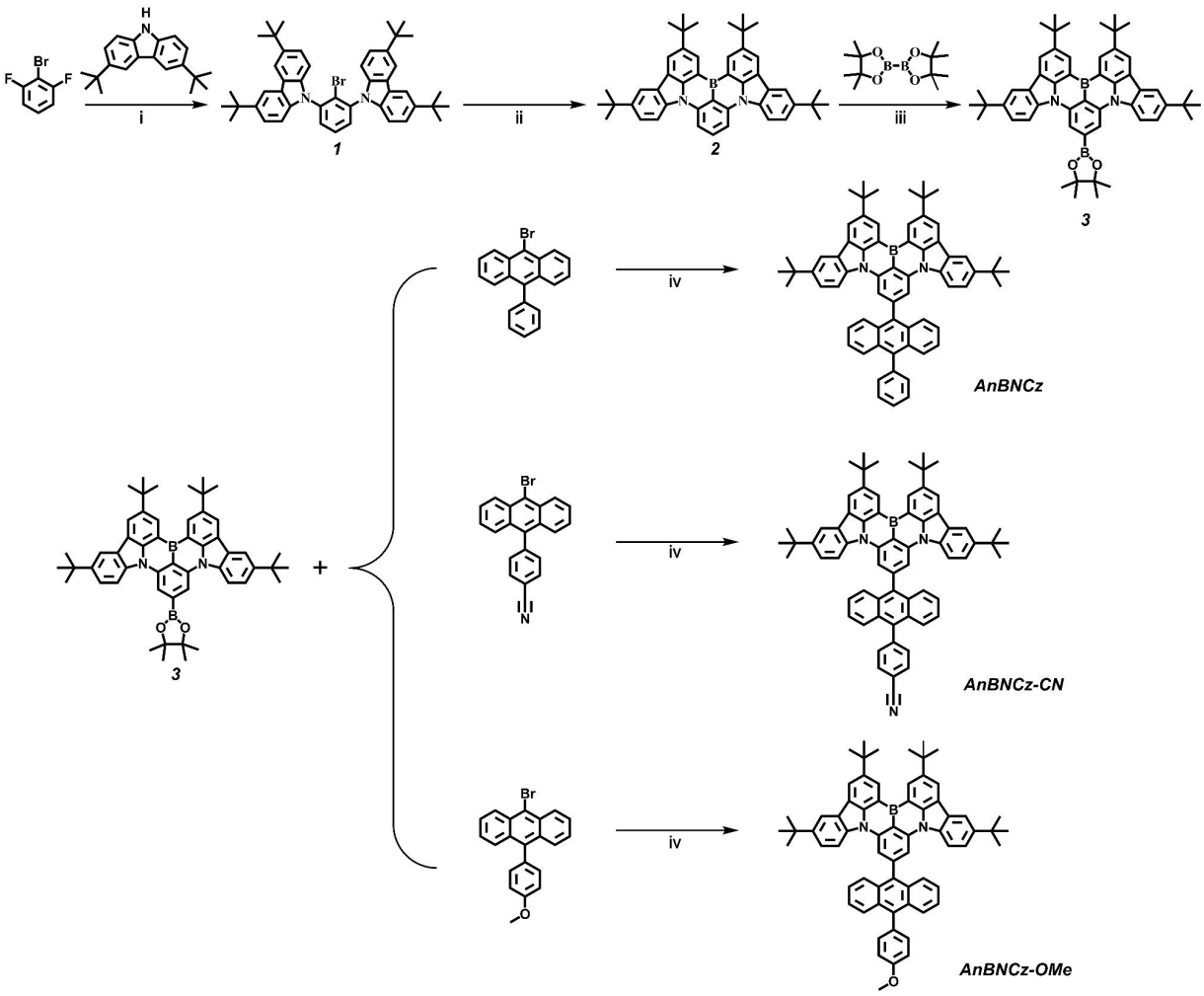

Scheme S1. Synthetic procedures of **AnBNCz**, **AnBNCz-CN** and **AnBNCz-OMe**: i) Cs_2CO_3, DMF, 150 °C, 12 h; ii) 1. *n*-BuLi, *t*-BuPh, 0 °C, 30 min, then 60 °C, 2 h; 2. BBr_3, -10°C, 1 h, then RT, 0.5 h; 3. $NEt(i\text{-}Pr)_2$, -10 °C, then 120 °C, 7 h; iii) B_2pin_2, $[Ir(cod)OMe]_2$, dtbpy, THF, 75 °C, 24 h; iv) $Pd(PPh_3)_4$, K_2CO_3, Toluene/C_2H_5OH/H_2O, reflux, 100 °C, 24 h.

Preparation for ***1***, ***2*** and ***3*** were referred to the reported procedures.[2,3]

Synthesis of **AnBNCz**: To a 100 mL round bottom flask with a reflux condenser were placed ***3*** (0.50 g, 0.65 mmol), 9-bromo-10-phenylanthracene (0.22 g, 0.66 mmol), $Pd(PPh_3)_4$ (38.00 mg, 0.033 mmol) and K_2CO_3 (1.38 g, 1.00 mmol). The flask was vacuumed and purged with dry nitrogen by three times. Toluene (20 mL), C_2H_5OH (10 mL) and deionized water (10

mL) were then injected into the flask. The reaction mixture was refluxed for 24 h under a nitrogen atmosphere. After cooling to room temperature, the mixture was poured into water and extracted with dichloromethane. The combined organic extracts were dried over anhydrous magnesium sulfate, and subsequently filtered and evaporated the solvent. The crude product was purified by silica-gel column chromatography using petroleum ether/dichloromethane as eluent. **AnBNCz** was obtained as a yellow solid in 75% yield (0.30 g). ^{1}H NMR (400 MHz, Chloroform-*d*) δ 9.22 (d, J = 1.9 Hz, 2H), 8.51 – 8.50 (m, 4H), 8.25 (d, J = 2.0 Hz, 2H), 8.17 (d, J = 8.9 Hz, 2H), 8.00 – 7.97 (m, 2H), 7.82 – 7.79 (m, 2H), 7.70 – 7.66 (m, 2H), 7.62 – 7.60 (m, 2H), 7.44 (dd, J = 8.8, 2.1 Hz, 2H), 7.42 – 7.33 (m, 5H), 1.71 (s, 18H), 1.44 (s, 18H). ^{13}C NMR (101 MHz, Chloroform-*d*) δ 144.38, 143.83, 143.47, 143.32, 140.73, 138.03, 137.24, 136.69, 136.13, 130.35, 128.96, 128.87, 127.47, 126.57, 126.07, 126.02, 125.99, 124.53, 124.20, 123.40, 122.77, 119.77, 116.12, 113.26, 110.17, 34.21, 33.69, 31.20, 30.70, 28.67. HRMS (APCI): calcd for $C_{66}H_{61}BN_2$ $[M+H]^+$ 893.49, found 893.5006.

Synthesis of **AnBNCz-CN**: This compound was synthesized in a procedure similar to that for **AnBNCz**. **AnBNCz-CN** was obtained as a yellow solid (Yield: 72%). ^{1}H NMR (400 MHz, Chloroform-*d*) δ 9.23 (d, J = 1.9 Hz, 2H), 8.51 (d, J = 1.8 Hz, 2H), 8.48 (s, 2H), 8.25 (d, J = 2.1 Hz, 2H), 8.15 (d, J = 8.9 Hz, 2H), 8.02 – 7.98 (m, 4H), 7.76 – 7.73 (m, 2H), 7.66 – 7.64 (m, 2H), 7.41 (ddt, J = 13.5, 8.5, 1.5 Hz, 6H), 1.72 (s, 18H), 1.44 (s, 18H). ^{13}C NMR (101 MHz, Chloroform-*d*) δ 144.47, 143.94, 143.49, 143.35, 142.95, 140.72, 137.28, 137.20, 134.06, 131.38, 131.32, 128.90, 128.80, 128.48, 126.29, 126.07, 125.12, 124.94, 124.75, 123.35, 122.78, 120.70, 119.85, 117.90, 116.20, 113.15, 110.74, 109.96, 34.21, 33.70, 31.19, 30.69. HRMS (APCI): calcd for $C_{67}H_{60}BN_3$ $[M+H]^+$ 918.49, found 918.4954.

Synthesis of **AnBNCz-OMe**: This compound was synthesized in a procedure similar to that for **AnBNCz**. **AnBNCz-OMe** was obtained as a yellow solid (Yield: 72%). ^{1}H NMR (400 MHz, Chloroform-*d*) δ 9.22 (d, J = 1.9 Hz, 2H), 8.52 – 8.47 (m, 4H), 8.24 (d, J = 2.0 Hz, 2H), 8.17 (d, J = 8.9 Hz, 2H), 7.97 (dd, J = 8.2, 1.6 Hz, 2H), 7.87 – 7.83 (m, 2H), 7.54 – 7.50 (m, 2H), 7.44 – 7.33 (m, 6H), 7.23 – 7.19 (m, 2H), 4.00 (s, 3H), 1.71 (s, 18H), 1.44 (s, 18H). ^{13}C NMR (101 MHz, Chloroform-*d*) δ 158.11, 144.37, 143.82, 143.53, 143.32, 140.73, 137.24, 136.50, 135.96, 131.41, 130.04, 129.30, 128.91, 128.86, 126.15, 126.01, 125.99, 124.51, 124.12, 123.39, 122.77, 120.72, 119.76, 116.11, 113.26, 112.94, 110.19, 54.40, 34.20, 33.69, 31.20, 30.70. HRMS (APCI): calcd for $C_{67}H_{63}BN_2O$ $[M+H]^+$ 923.50, found 923.5113.

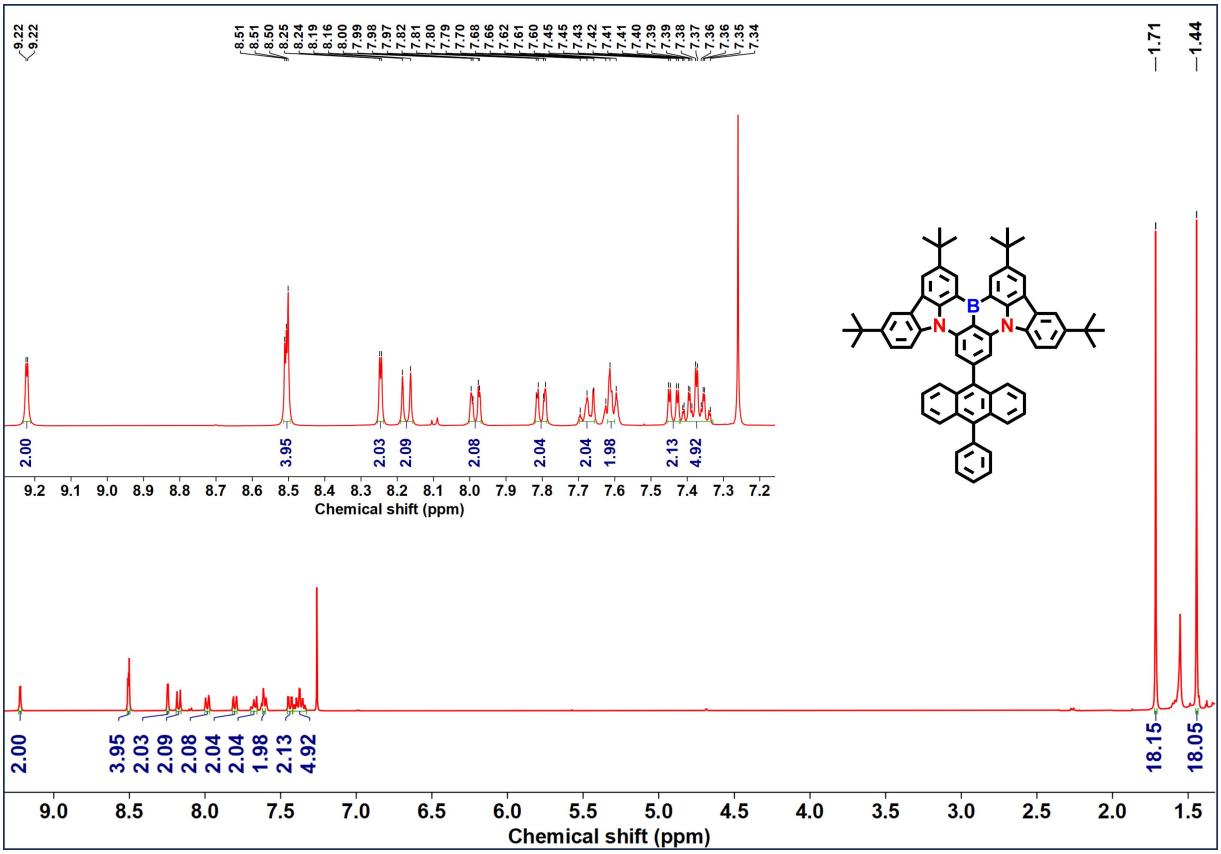

Fig. S1. [1]H NMR spectrum of **AnBNCz**.

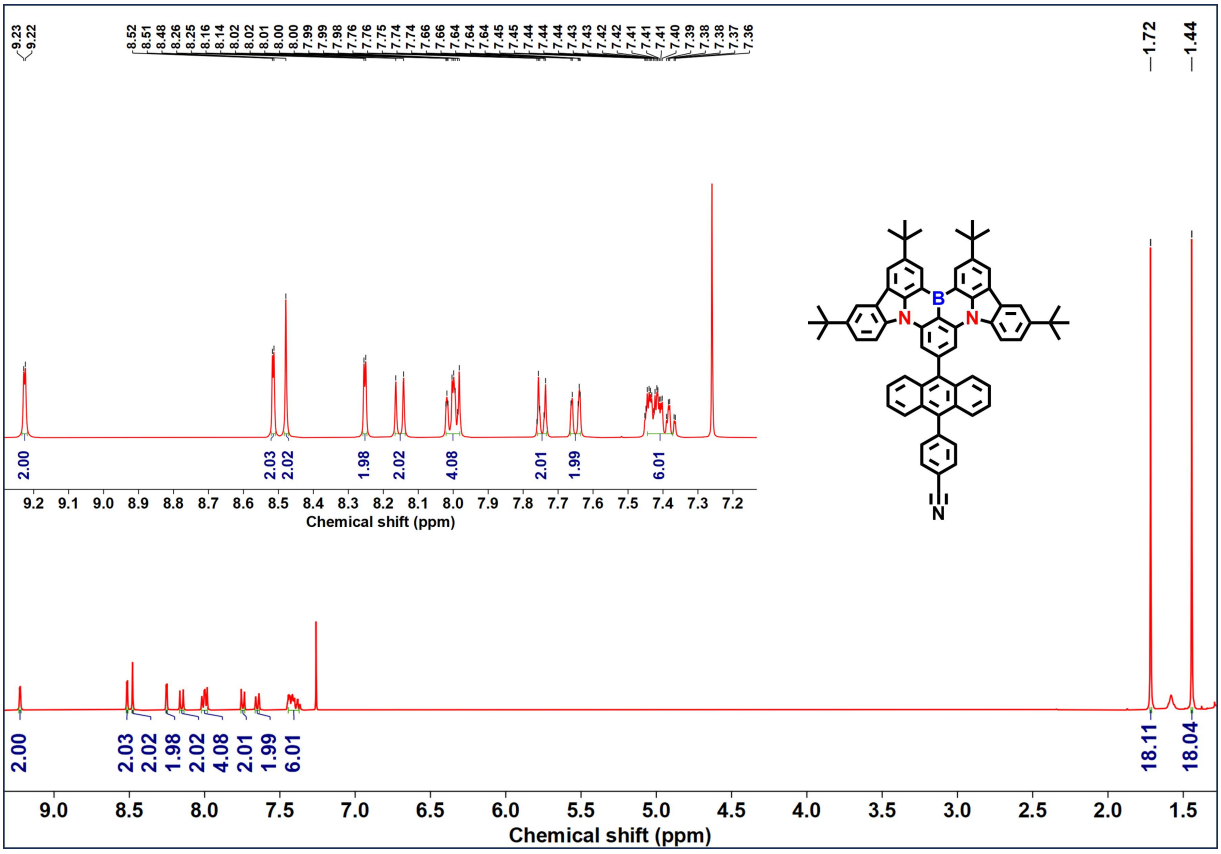

Fig. S2. [1]H NMR spectrum of **AnBNCz-CN**.

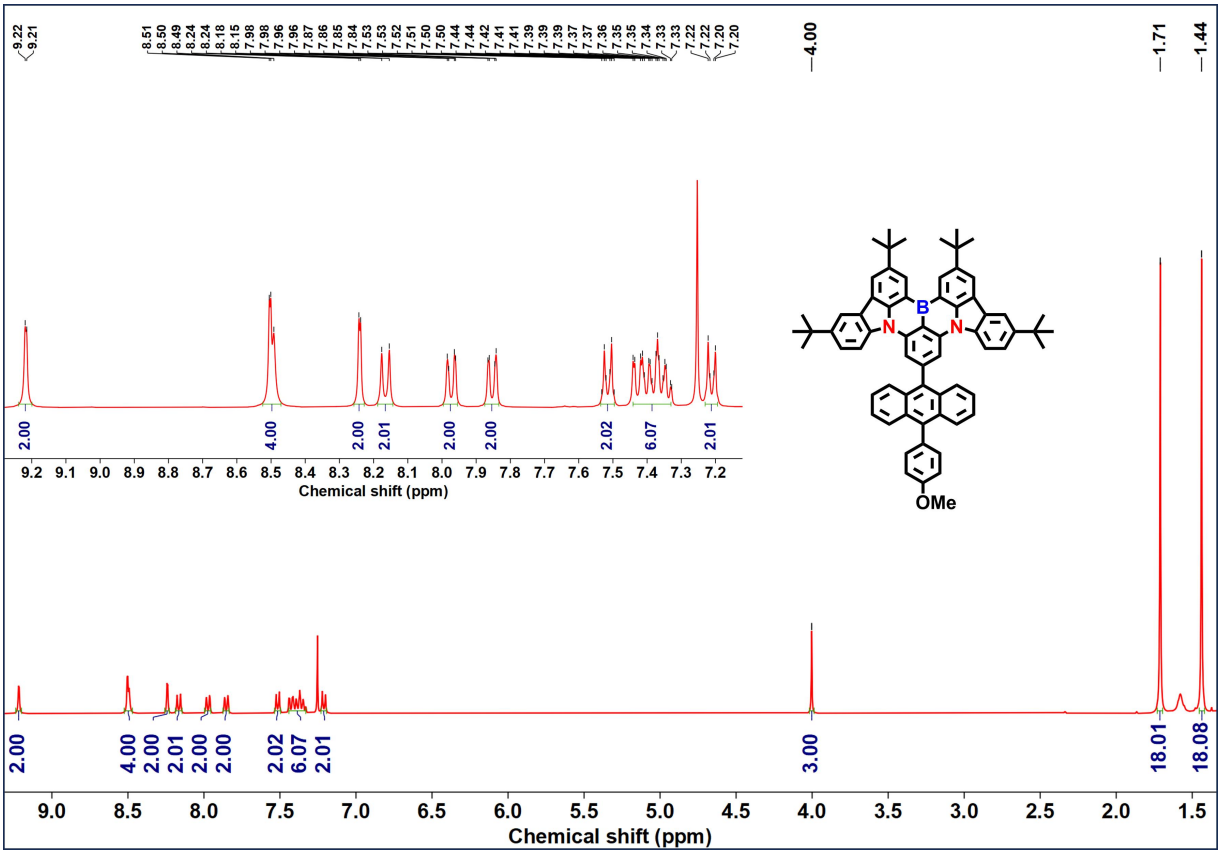

Fig. S3. ^{1}H MR spectrum of **AnBNCz-OMe**.

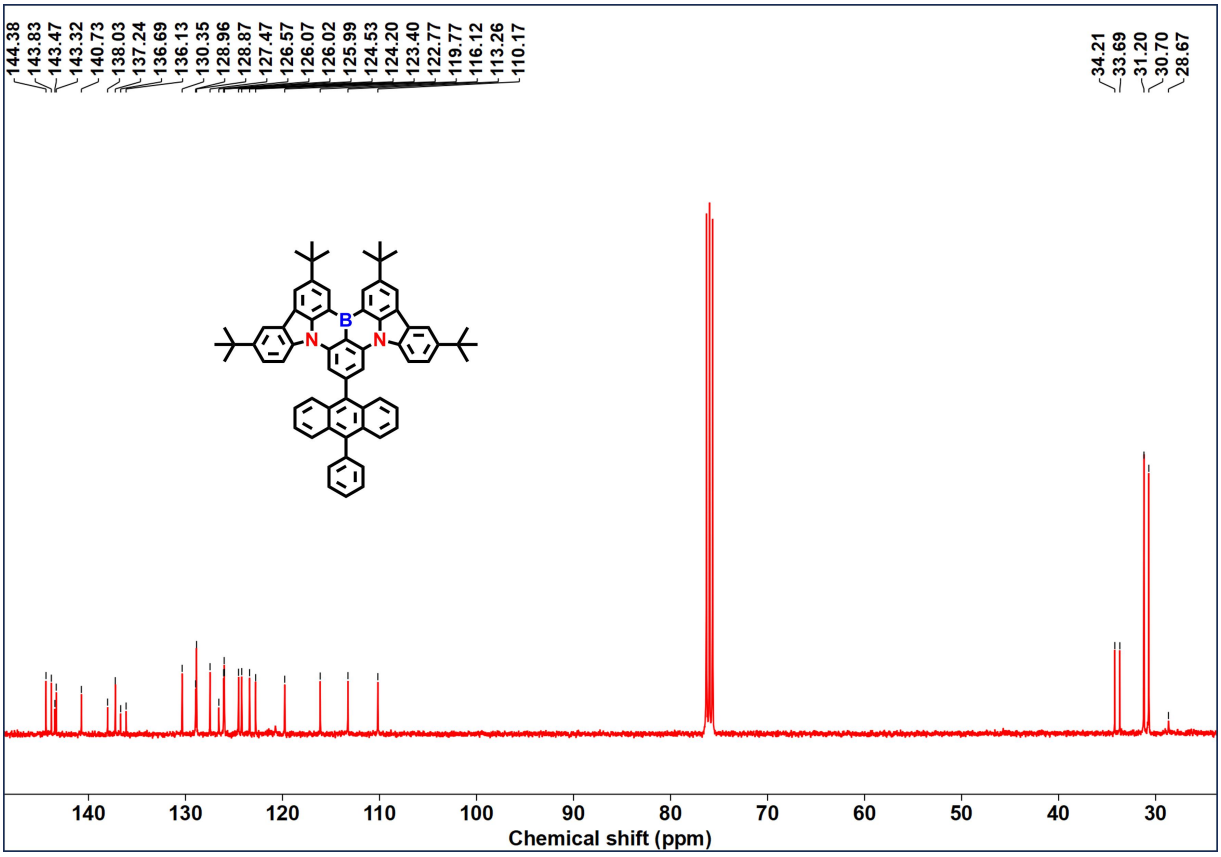

Fig. S4. ^{13}C MR spectrum of **AnBNCz**.

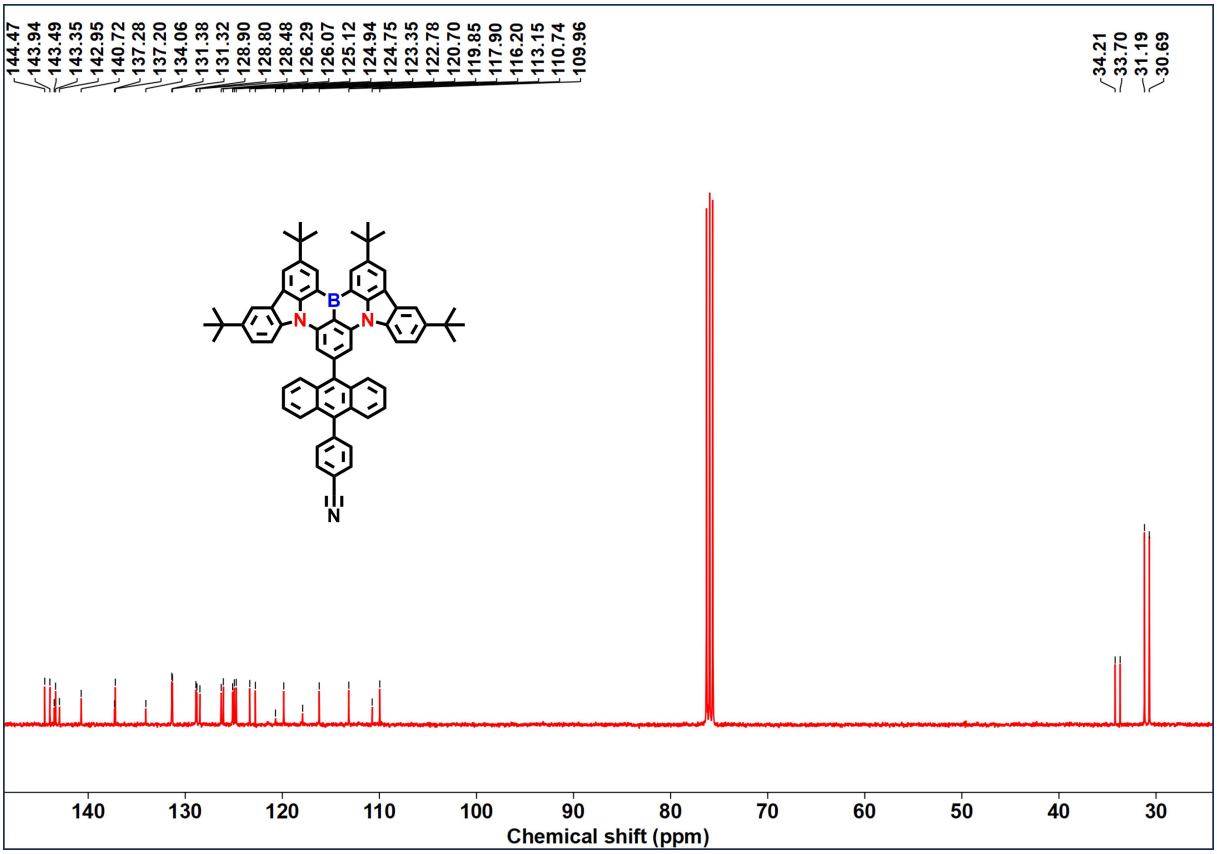

Fig. S5. ^{13}C MR spectrum of **AnBNCz-CN**.

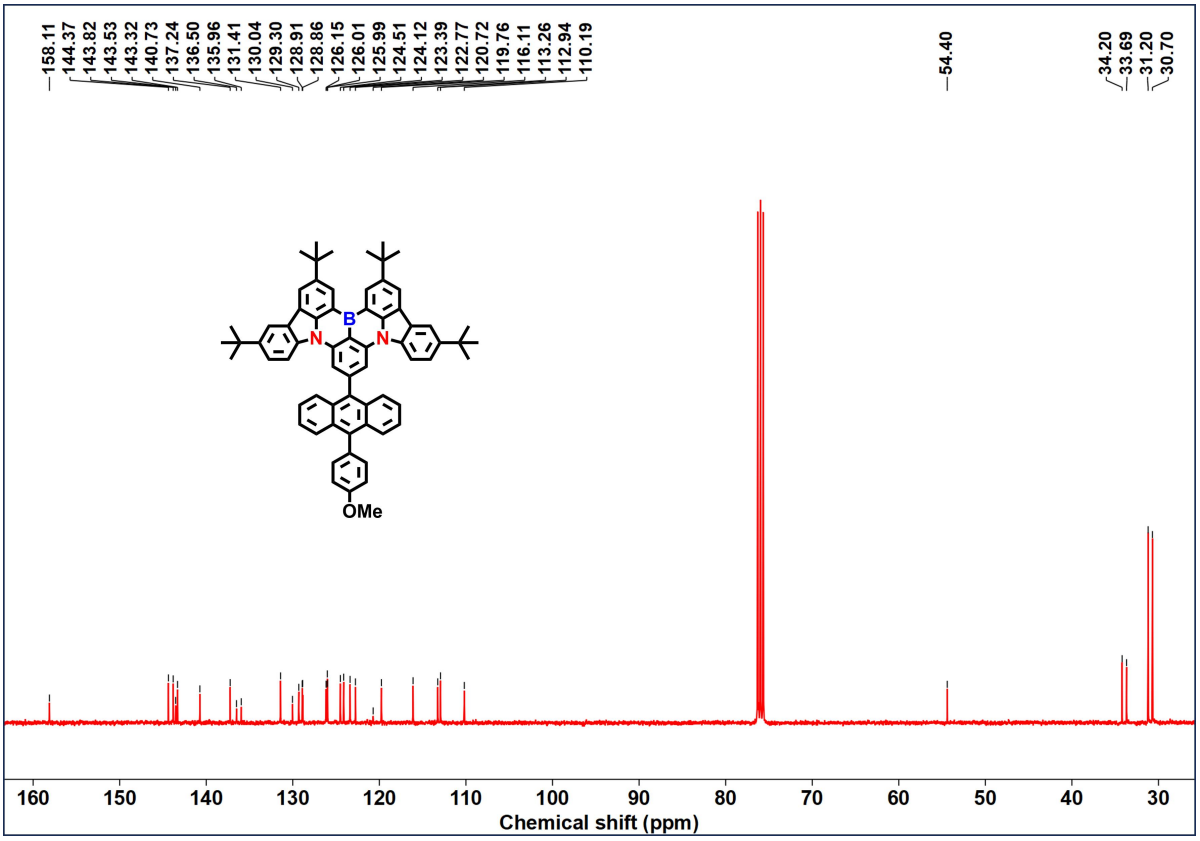

Fig. S6. ^{13}C MR spectrum of **AnBNCz-OMe**.

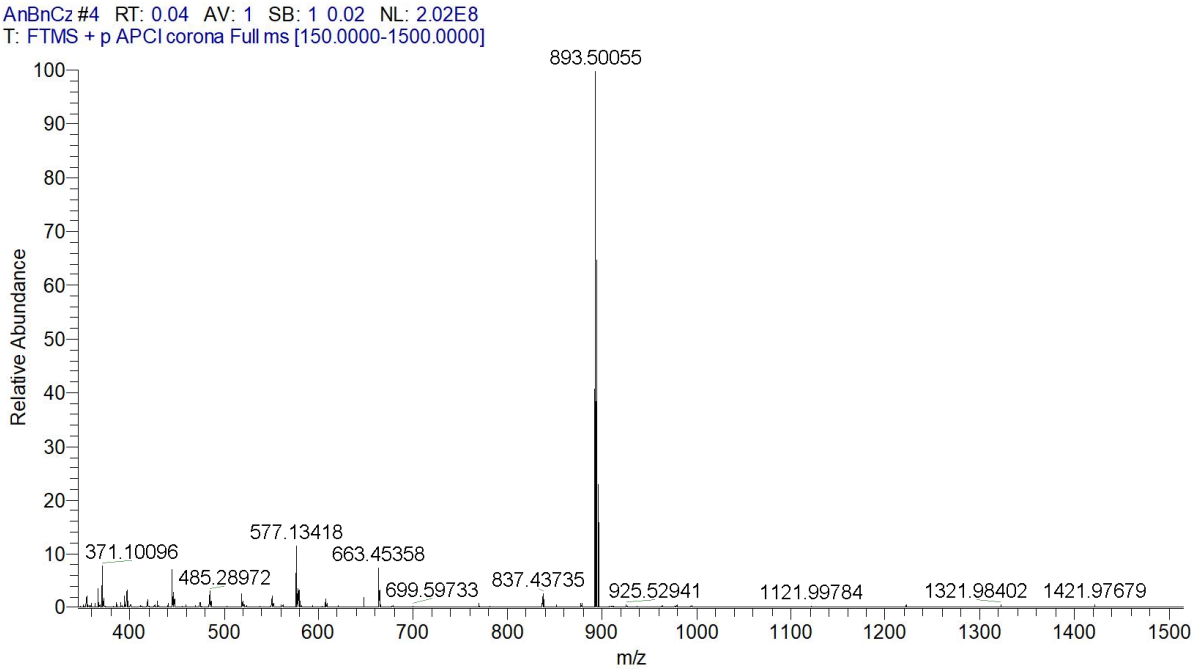

Fig. S7. HRMS spectrum of **AnBNCz**.

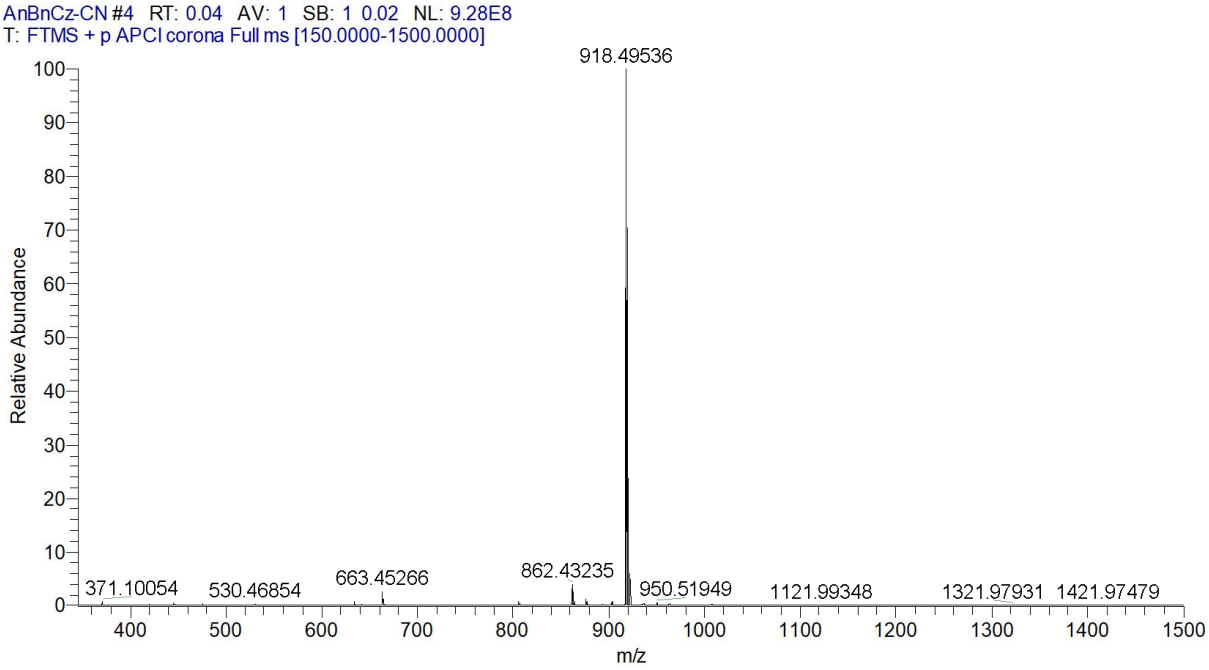

Fig. S8. HRMS spectrum of **AnBNCz-CN**.

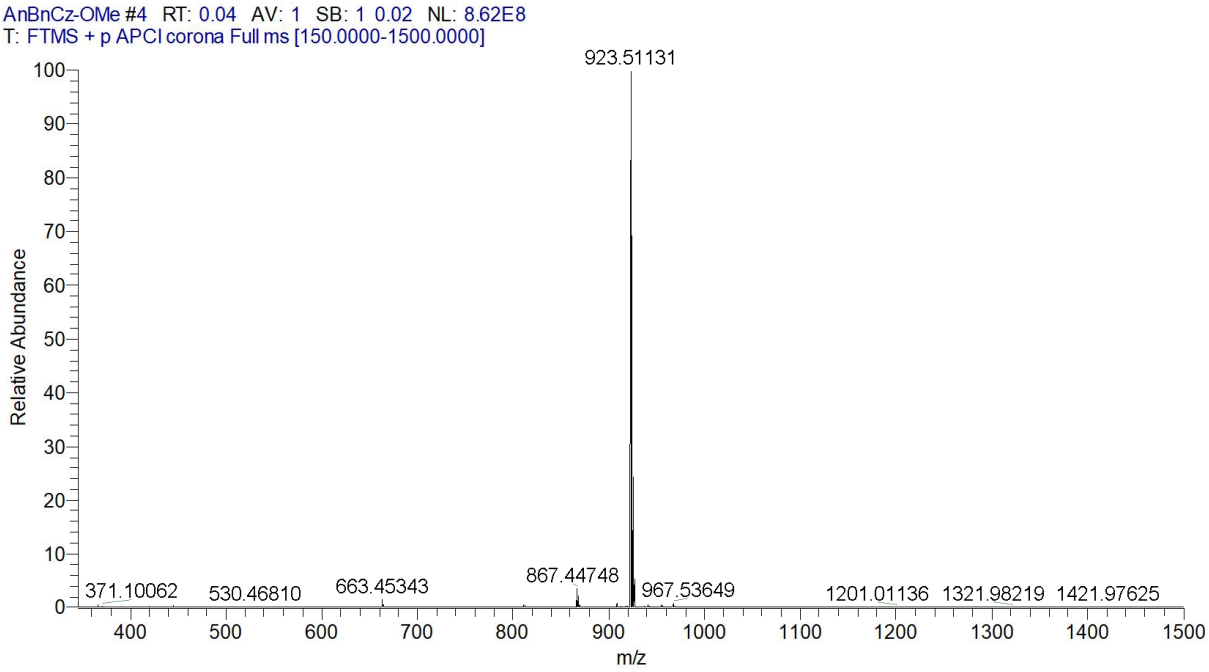

Fig. S9. HRMS spectrum of **AnBNCz-OMe**.

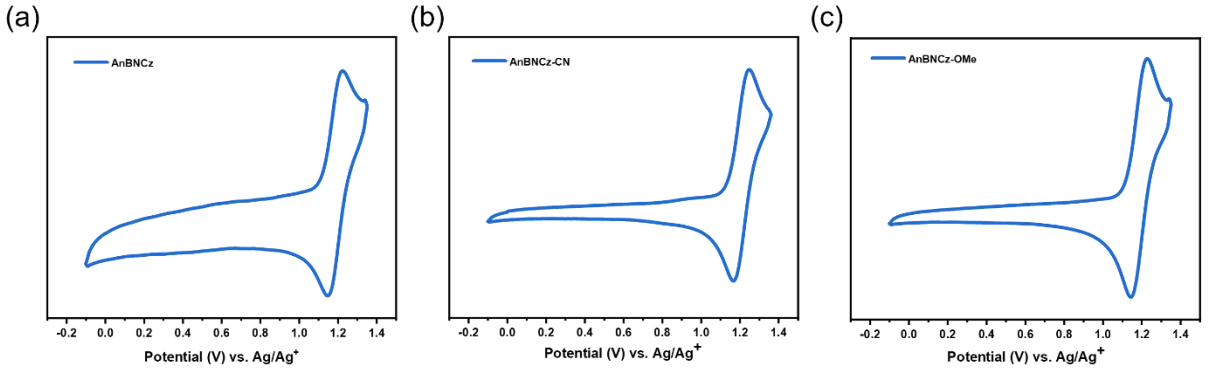

Fig. S10. Cyclic voltammograms cures of (a) **AnBNCz**, (b) **AnBNCz-CN** and (c) **AnBNCz-OMe**.

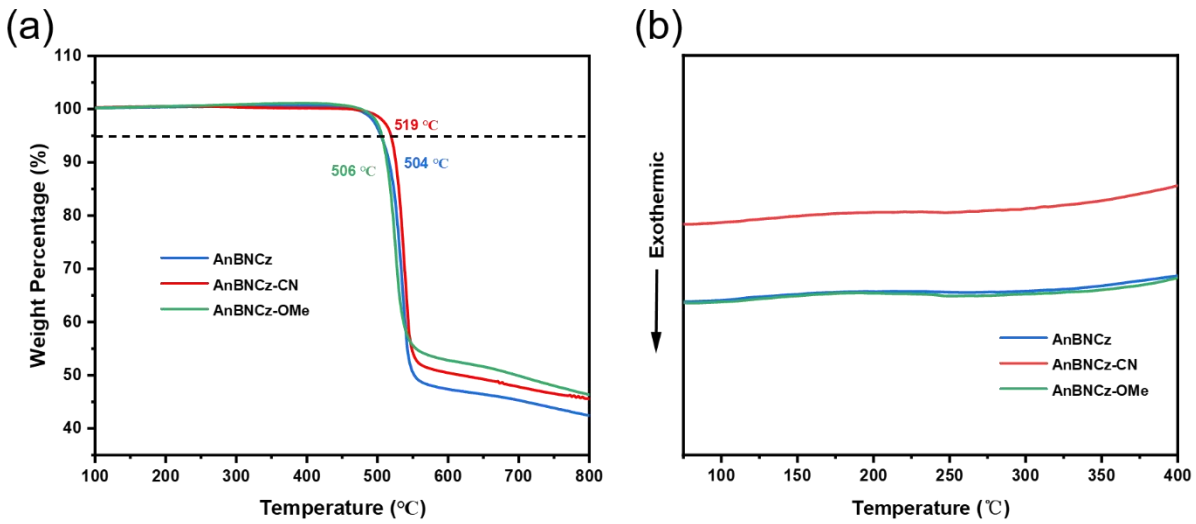

Fig. S11. (a) TGA and (b) DSC curves of **AnBNCz**, **AnBNCz-CN** and **AnBNCz-OMe**.

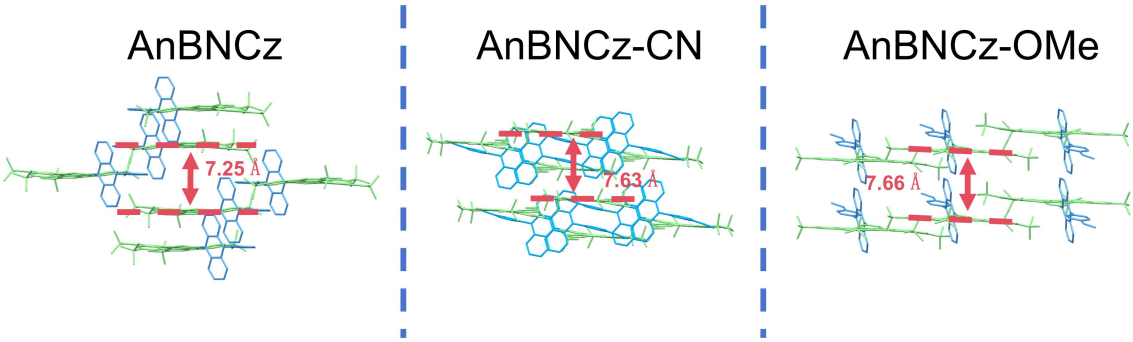

Fig. S12. X-ray crystal structures of **AnBNCz**, **AnBNCz-CN** and **AnBNCz-OMe**.

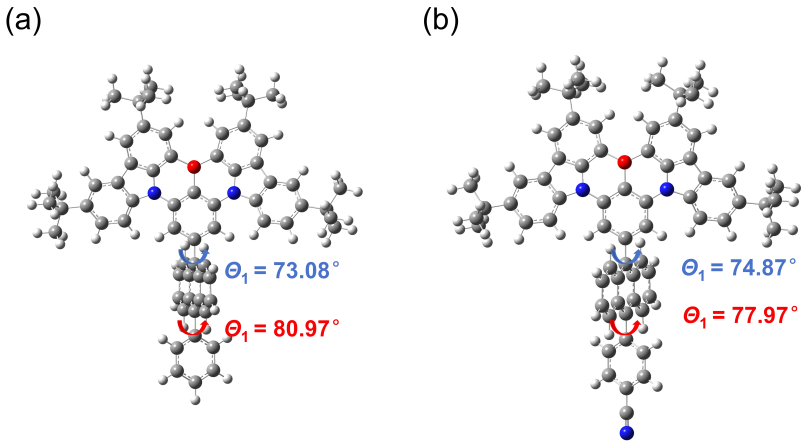

Fig. S13. Optimized geometry structures of (a) **AnBNCz** and (b) **AnBNCz-CN**.

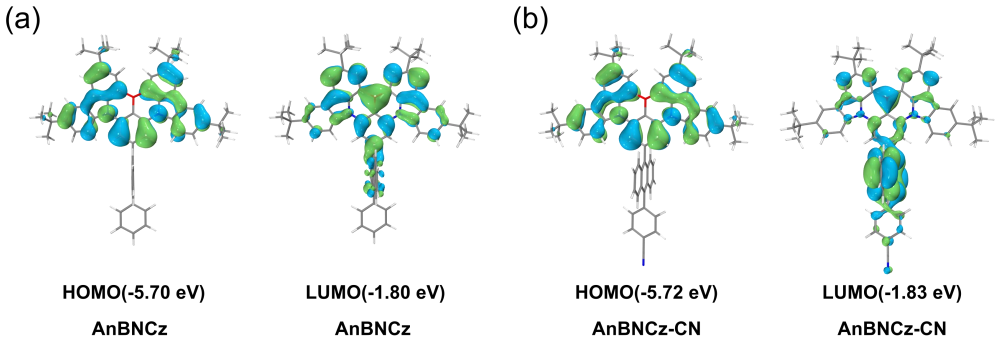

Fig. S14. The frontier molecular orbital distributions (FMOs) of (a) **AnBNCz** and (b) **AnBNCz-CN**.

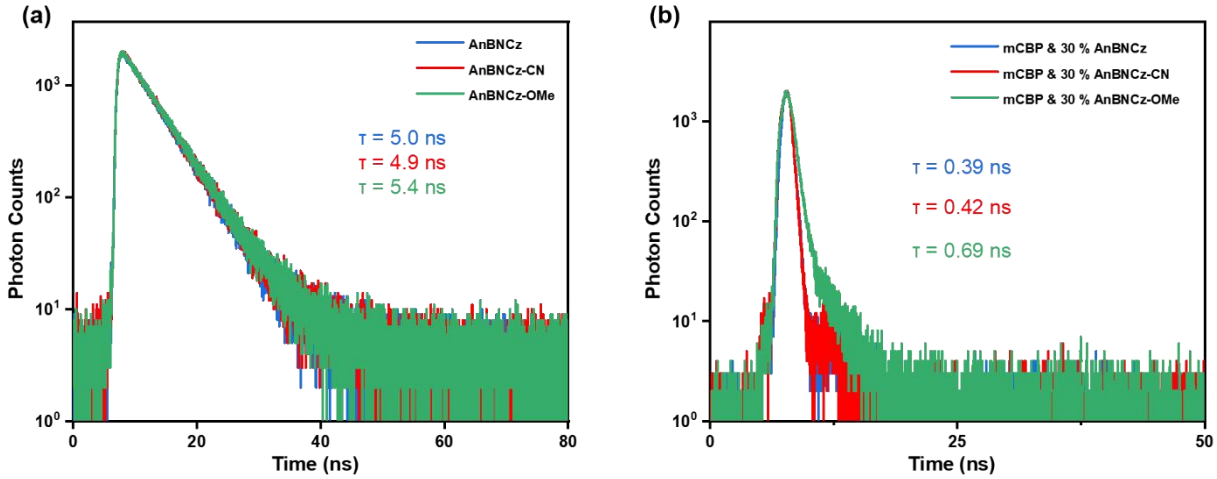

Fig. S15. (a) The transient PL decay spectra of **AnBNCz**, **AnBNCz-CN** and **AnBNCz-OMe** in dilute toluene and the doped films (b).

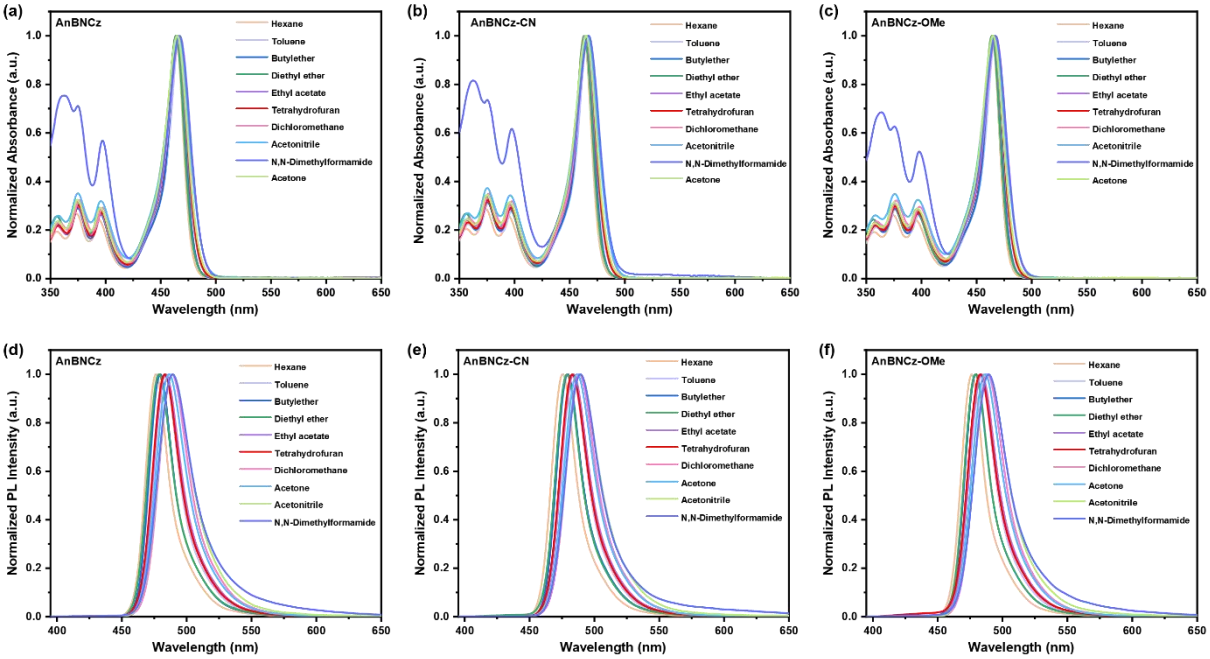

Fig. S16. Absorption spectra of (a) **AnBNCz**, (b) **AnBNCz-CN** and (c) **AnBNCz-OMe** dissolved in different polar solvents (10^{-5} M). PL spectra of (d) **AnBNCz**, (e) **AnBNCz-CN** and (f) **AnBNCz-OMe** dissolved in different polar solvents (10^{-5} M).

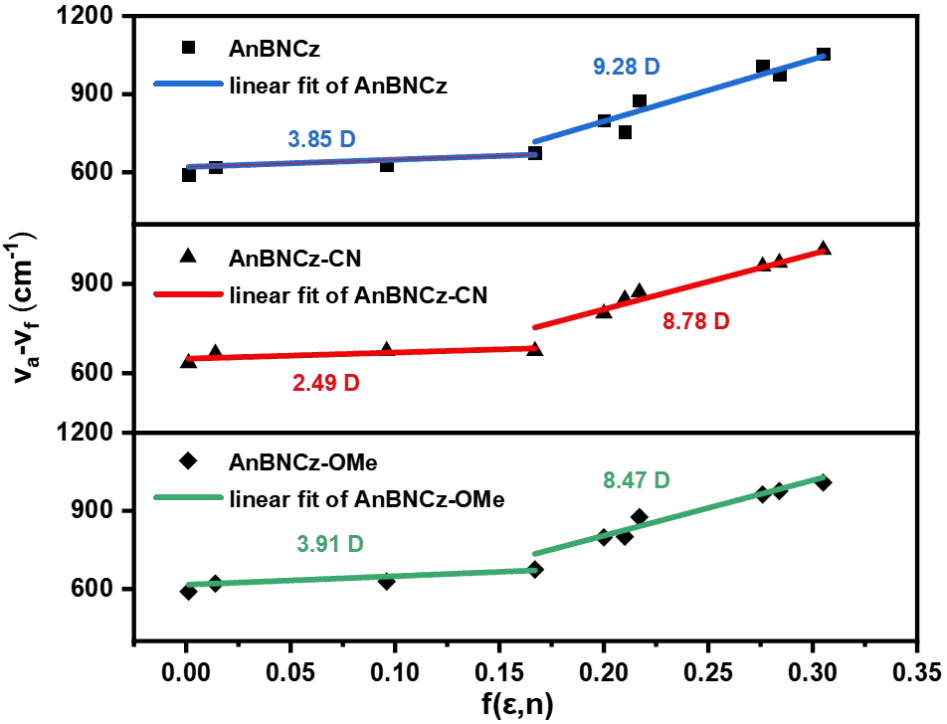

Fig. S17. Lippert–Mataga plots of the fluorescence maxima of **AnBNCz**, **AnBNCz-CN** and **AnBNCz-OMe** against the solvent polarity parameters.

Kinetic Analysis

The k_r, k_{nr} represent the decay rate constants of radiative and nonradiative processes, determined by the following formula:[4]

$\tau_F = 1 / (k_r + k_{nr})$

$\Phi_{PL} = k_r / (k_r + k_{nr})$

$k_r = \Phi_{PL} / \tau_F$

$k_{nr} = 1 / \tau_F - k_r$

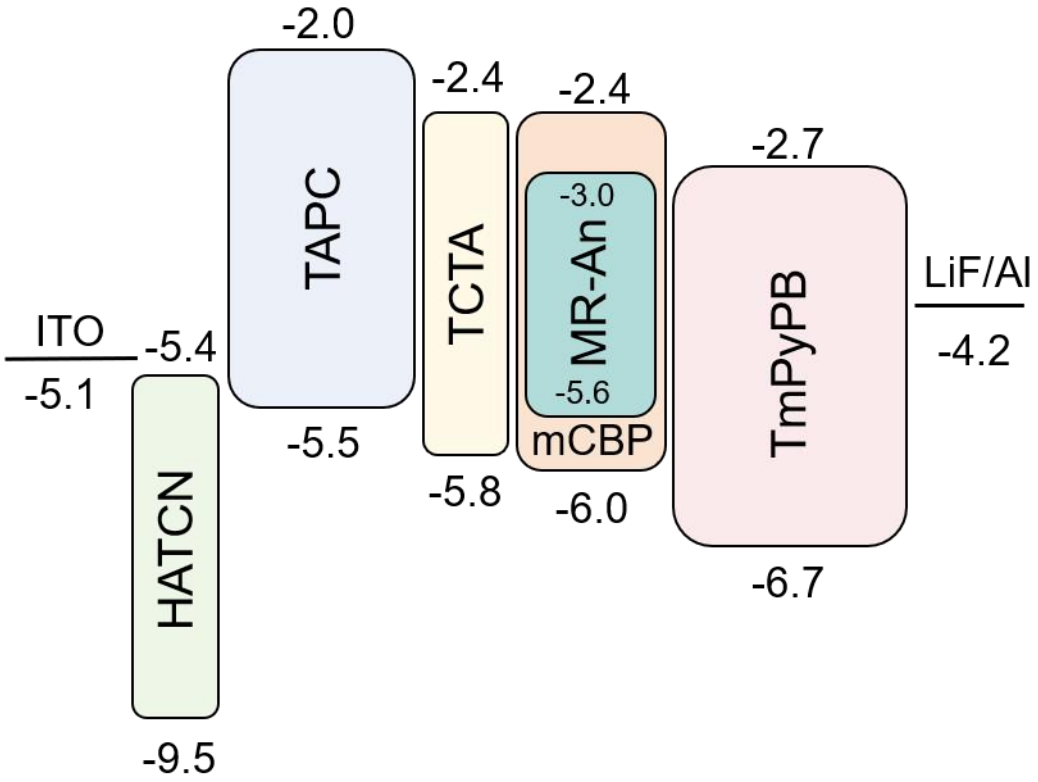

Fig. S18. Device architecture and energy-level diagram of the functional materials for OLEDs.

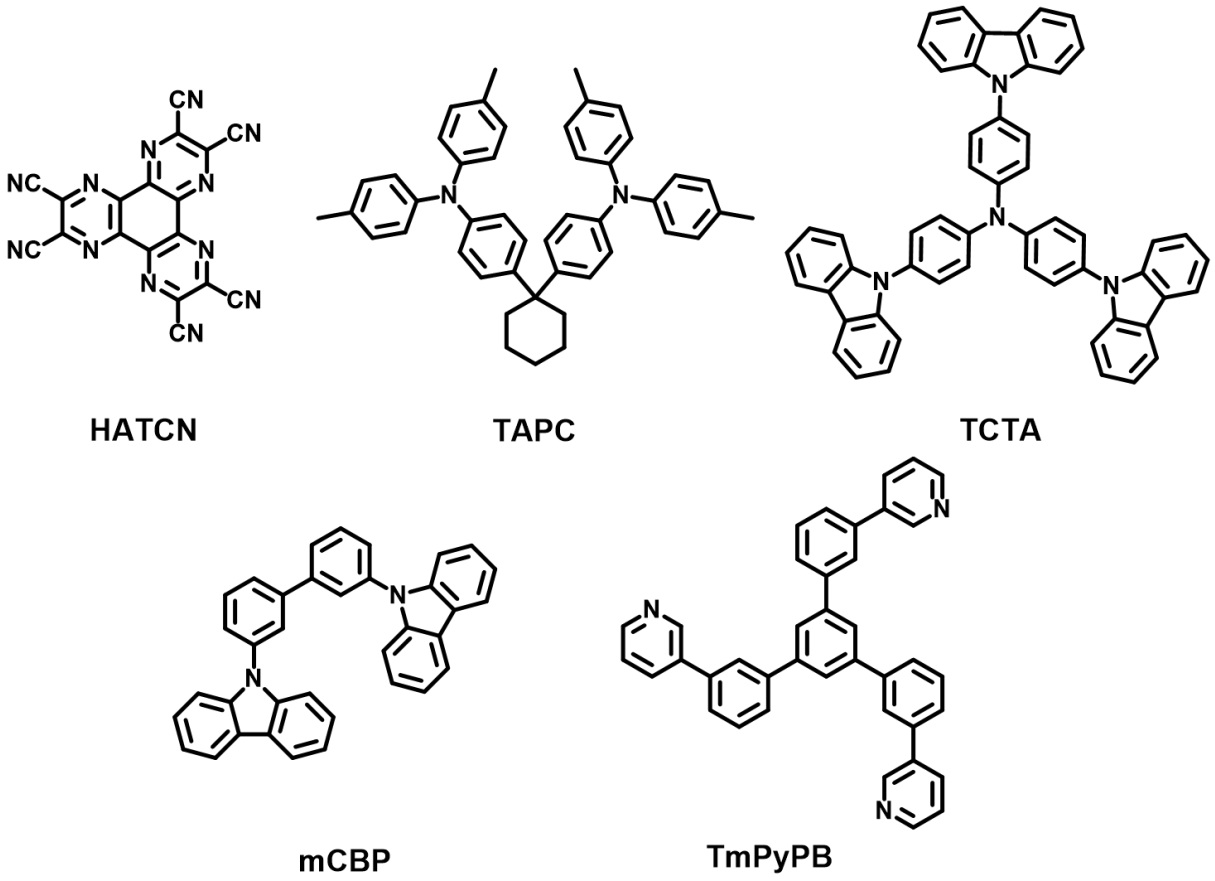

Fig. S19. Chemical structures of the OLED materials

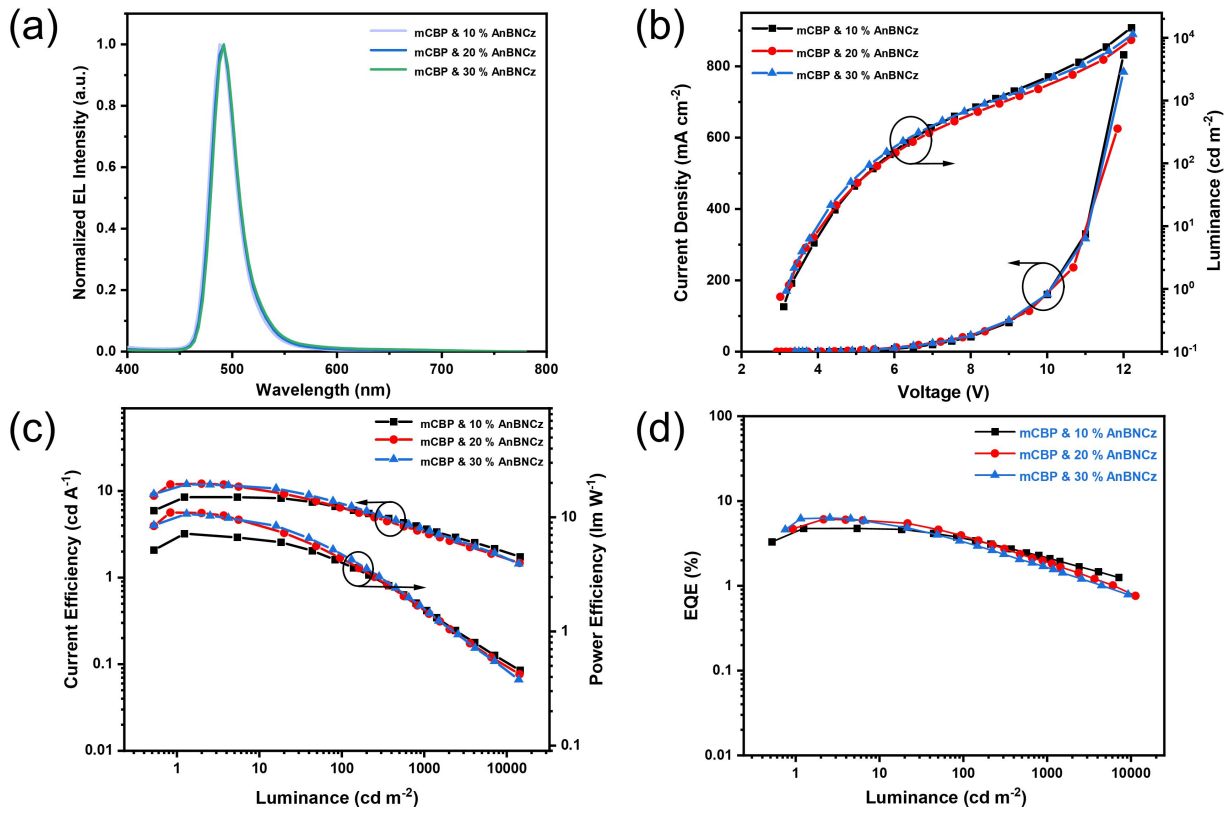

Fig. S20. (a) EL spectra, (b) changes in luminance and current density with applied voltage, (c) current efficiency-luminance and power efficiency-luminance characteristics, and (d) plot of EQE versus luminescence the **AnBNCz**-based doped devices at different dopant concentrations.

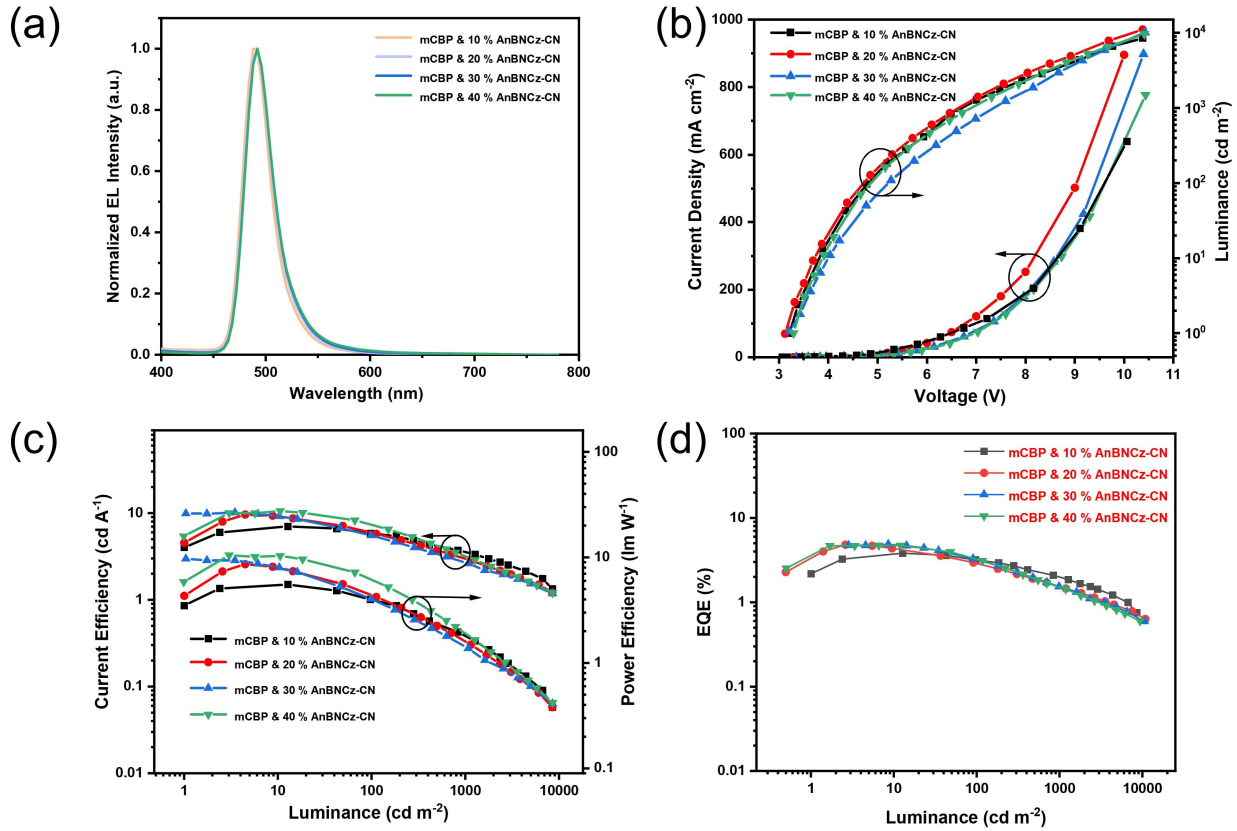

Fig. S21. (a) EL spectra, (b) changes in luminance and current density with applied voltage, (c) current efficiency-luminance and power efficiency-luminance characteristics, and (d) plot of EQE versus luminescence the **AnBNCz-CN**-based doped devices at different dopant concentrations.

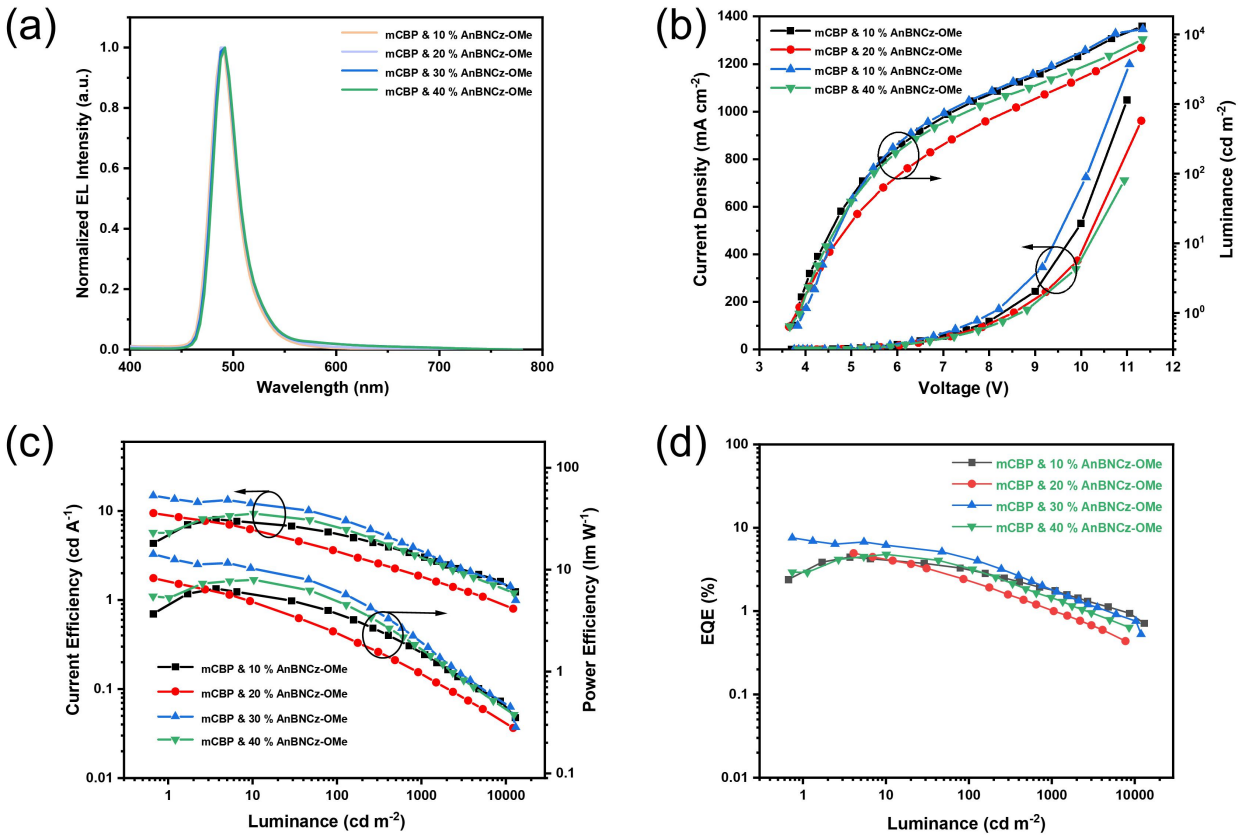

Fig. S22. (a) EL spectra, (b) changes in luminance and current density with applied voltage, (c) current efficiency-luminance and power efficiency-luminance characteristics, and (d) plot of EQE versus luminescence the **AnBNCz-OMe**-based doped devices at different dopant concentrations.

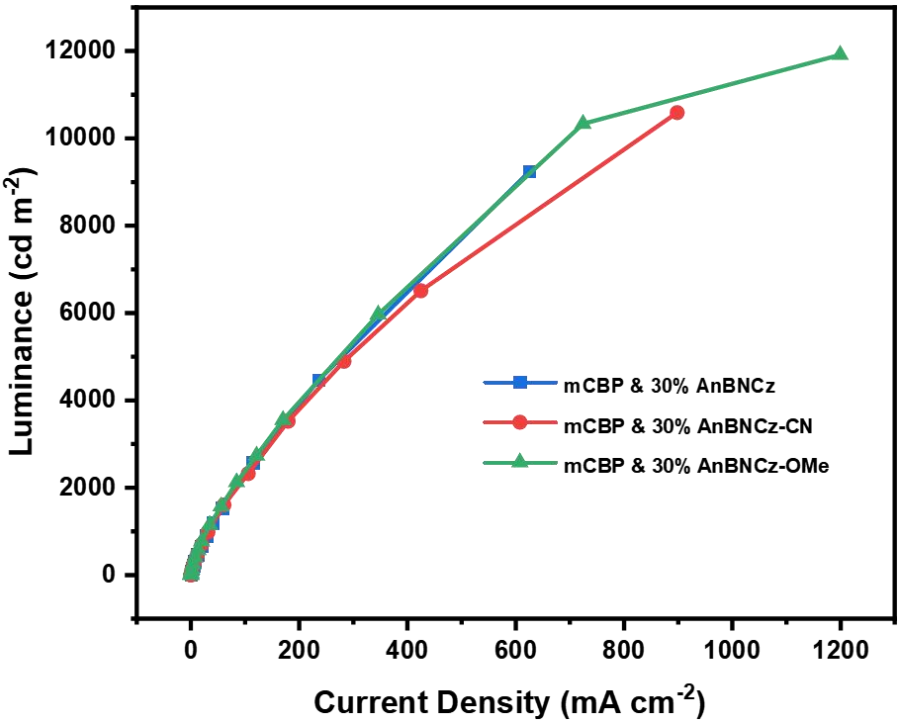

Fig. S23. Current density-luminance curve of the doped devices.

As for the TTA mechanism device, the brightness should increase exponentially over current density,[5] which is noticeably different from the doped device. This can exclude the contribution from TTA process of **AnBNCz**, **AnBNCz-CN** and **AnBNCz-OMe**.

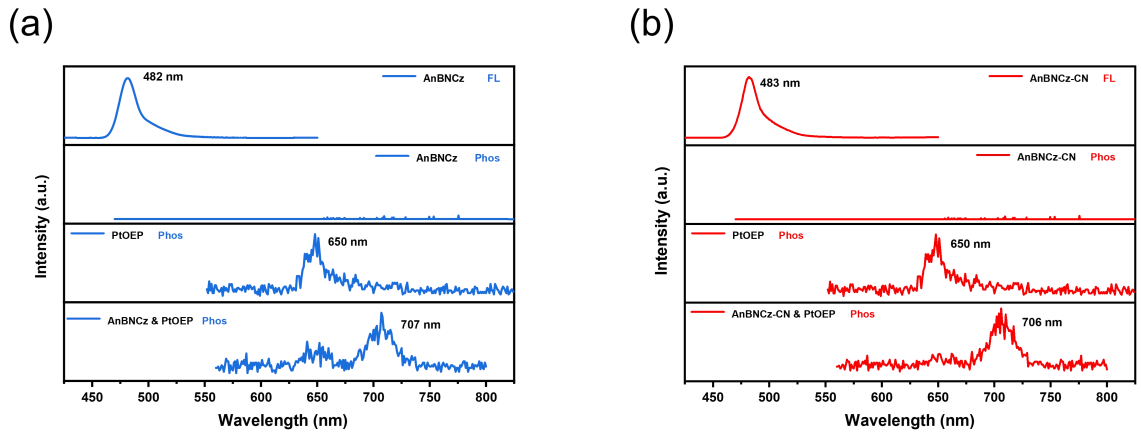

Fig. S24. (a) / (b) Fluorescence spectrum of the **AnBNCz** / **AnBNCz-CN** solution and 20 ms delayed phosphorescence spectra of **AnBNCz**/**AnBNCz-CN**, **PtOEP** and **AnBNCz & PtOEP**/ **AnBNCz-CN & PtOEP** solution at 77 K.

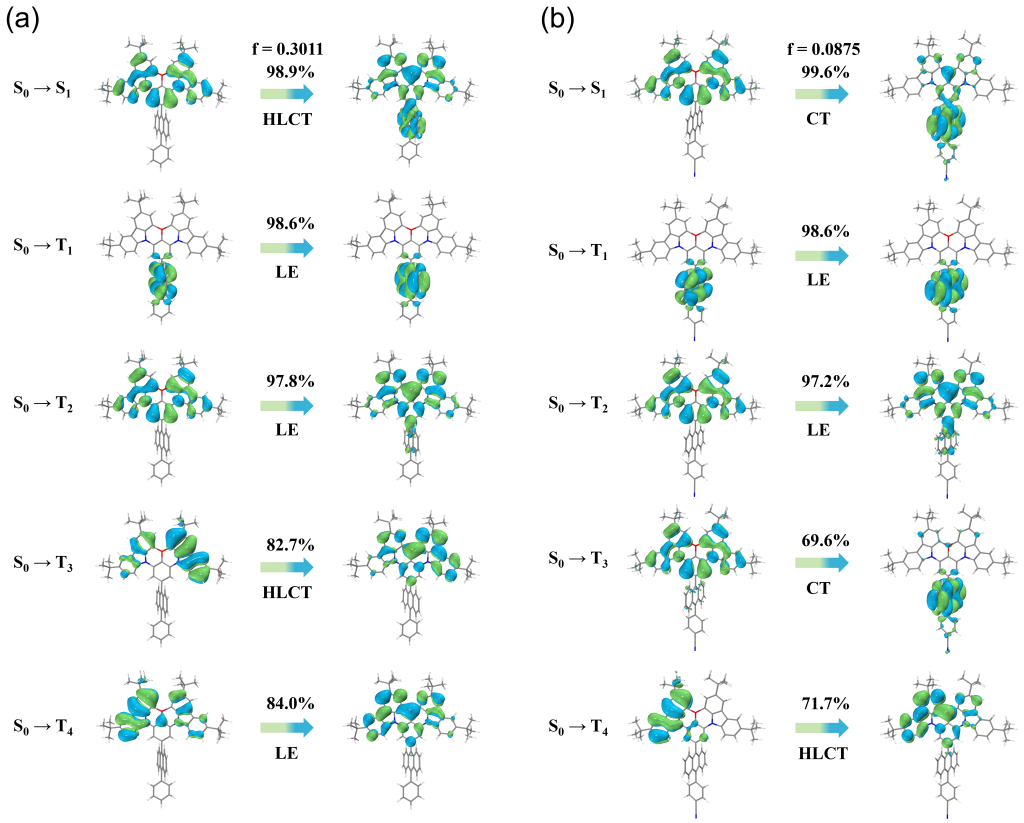

Fig. S25. (a) Natural transition orbitals of **AnBNCz**, (b) Natural transition orbitals of **AnBNCz-CN**.

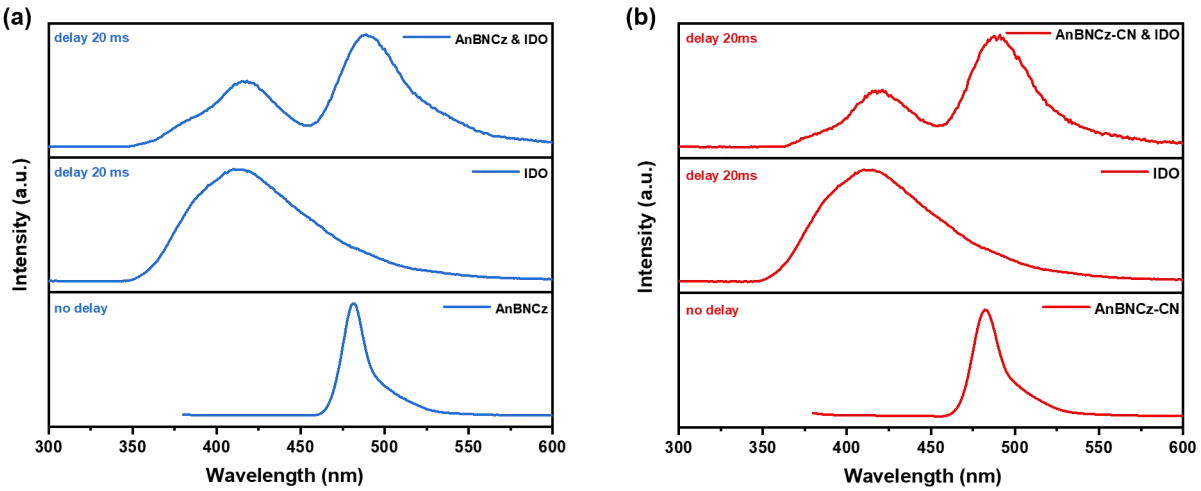

Fig. S26. (a) The top: 20 ms delayed PL spectra of the **AnBNCz & IDO** solution; the middle: 20 ms delayed phosphorescence spectra of **IDO**. The PL spectra of **AnBNCz** at 77 K appear at the bottom of (a); (b) The top: 20 ms delayed PL spectra of the **AnBNCz-CN & IDO** solution; the middle: 20 ms delayed phosphorescence spectra of **IDO**. The PL spectra of **AnBNCz-CN** at 77 K appear at the bottom of (b). (In the ketones-sensitized solution, the concentration of the ketones and the acceptors were 10^{-6} M and 10^{-4} M, respectively.)

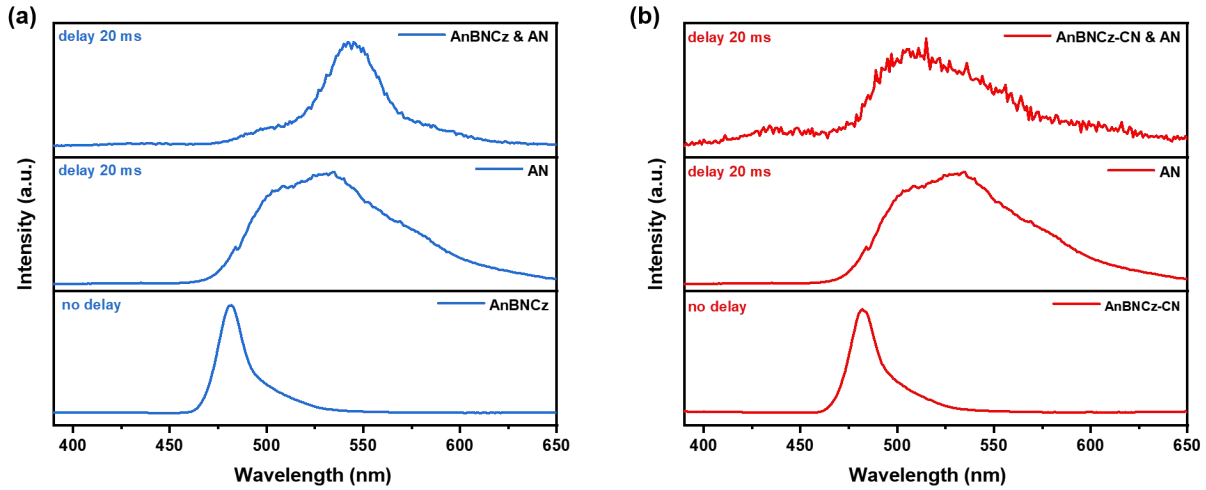

Fig. S27. (a) The top: 20 ms delayed PL spectra of the **AnBNCz & AN** solution; the middle: 20 ms delayed phosphorescence spectra of **AN**. The PL spectra of **AnBNCz** at 77 K appear at the bottom of (a); (b) The top: 20 ms delayed PL spectra of the **AnBNCz-CN & AN** solution; the middle: 20 ms delayed phosphorescence spectra of **AN**. The PL spectra of **AnBNCz-CN** at 77 K appear at the bottom of (b). (In the ketones-sensitized solution, the concentration of the ketones and the acceptors were 10^{-6} M and 10^{-4} M, respectively.)

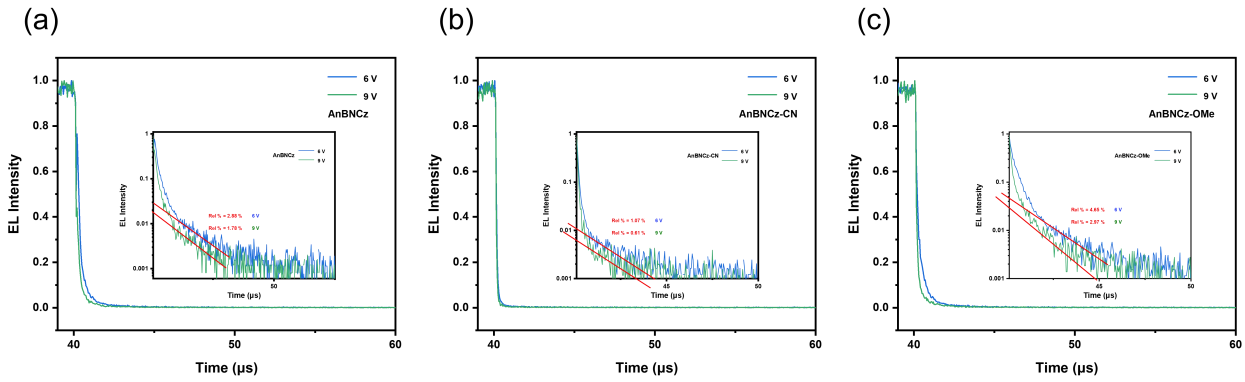

Fig. S28. Transient EL of the **AnBNCz-** (a), **AnBNCz-CN-** (b) and **AnBNCz-OMe-** (c) based OLEDs at different driven voltages.

Table S1. Summary of the crystallographic data of **AnBNCz**, **AnBNCz-CN** and **AnBNCz-OMe**.

Parameter	**AnBNCz**	**AnBNCz-CN**	**AnBNCz-OMe**
Empirical formula	$C_{78}H_{89}BN_2$	$C_{79}H_{88}BN_3$	$C_{78.769}H_{90.44}BN_2O$
Formula weight	1065.32	1090.33	1091.90
Temperature/K	150.00(10)	100.00(10)	237.15
Crystal system	monoclinic	triclinic	triclinic
Space group	*C*2/*c*	*P*-1	*P*-1

a/Å	19.0095(14)	8.70120(10)	8.6634(5)
b/Å	21.1707(15)	13.9528(2)	14.0107(7)
c/Å	15.7940(11)	27.8978(4)	27.9041(15)
α/°	90	94.4430(10)	94.565(2)
β/°	90.03(3)	97.9480(10)	98.146(2)
γ/°	90	104.1950(10)	103.370(2)
Volume/Å^3	6356.2(8)	3230.05(8)	3239.7(3)
Z	4	2	2
ρ_{calc}g/cm^3	1.113	1.121	1.119
μ/mm^{-1}	0.469	0.478	0.483
F(000)	2304.0	1176.0	1180.0
Crystal size/mm^3	0.17 × 0.14 × 0.12	0.15 × 0.13 × 0.12	0.17 × 0.14 × 0.12
Radiation	Cu Kα (λ = 1.54184)	Cu Kα (λ = 1.54184)	Cu Kα (λ = 1.54178)
2Θ range for data collection/°	6.248 to 133.194	6.442 to 146.716	7.612 to 136.602
Index ranges	-22 ≤ h ≤ 22, -25 ≤ k ≤ 21, -12 ≤ l ≤ 18	-10 ≤ h ≤ 10, -17 ≤ k ≤ 13, -34 ≤ l ≤ 33	-10 ≤ h ≤ 10, -16 ≤ k ≤ 16, 0 ≤ l ≤ 33
Reflections collected	13279	49198	11660
Independent reflections	5610 [R_{int} = 0.0391, R_{sigma} = 0.0367]	12592 [R_{int} = 0.0327, R_{sigma} = 0.0285]	11660 [R_{int} = 0.0857, R_{sigma} = 0.1066]
Data/restraints/parameters	5610/350/380	12592/694/726	11660/690/727
Goodness-of-fit on F^2	1.064	1.060	1.206
Final R indexes [I>=2σ (I)]	R_1 = 0.0909, wR_2 = 0.2686	R_1 = 0.0446, wR_2 = 0.1189	R_1 = 0.1062, wR_2 = 0.2931
Final R indexes [all data]	R_1 = 0.1018, wR_2 = 0.2848	R_1 = 0.0498, wR_2 = 0.1229	R_1 = 0.1221, wR_2 = 0.3149
Largest diff. peak/hole / e Å^{-3}	0.53/-0.52	0.47/-0.42	0.41/-0.34

Table S2. Detailed absorption and emission peak positions of **AnBNCz**, **AnBNCz-CN** and **AnBNCz-OMe** in different solvents.

Solvents	ε	n	f(ε,n)	**AnBNCz**			**AnBNCz-CN**			**AnBNCz-OMe**		
				λ_a (nm)	λ_f (nm)	ν_a-ν_f (cm^{-1})	λ_a (nm)	λ_f (nm)	ν_a-ν_f (cm^{-1})	λ_a (nm)	λ_f (nm)	ν_a-ν_f (cm^{-1})
Hexane	1.9	1.375	0.0012	463	476	590	462	476	634	463	476	590

Toluene	2.38	1.494	0.014	468	482	620	467	482	666	468	482	621
Butylether	3.08	1.399	0.096	465	479	629	464	479	675	465	479	629
Ethyl ether	4.34	1.352	0.167	464	479	675	464	479	675	464	479	675
Ethyl acetate	6.02	1.372	0.2	466	484	798	465	483	801	466	484	798
Tetrahydrofuran	7.58	1.407	0.21	466	483	755	465	482	848	465	483	801
Dichloromethane	8.93	1.424	0.217	468	488	876	469	489	872	468	488	876
Acetone	20.7	1.359	0.284	464	486	976	465	487	971	464	486	976
Dimethyl Formamide	37.0	1.427	0.276	466	489	1009	468	490	959	467	489	963
Acetonitrile	37.5	1.344	0.305	465	489	1055	465	488	1014	466	489	1009

Table S3. Key data of OLEDs based on **AnBNCz, AnBNCz-CN** and **AnBNCz-OMe** with different dopant concentrations.

Compounds	Conc. (wt%)	λ_{EL} (nm)[a]	V_{on} (V)[b]	L (cd m^{-2})[c]	η_C (cd A^{-1})[c]	η_P (lm W^{-1})[c]	η_{ext} (%)[c]	FWHM (nm)[d]
				maximum value				
AnBNCz	10	488	3.6	9165	8.5	7.2	5.0	28
	20	492	3.5	11313	11.9	10.7	6.0	28
	30	492	3.5	9240	12.1	11.0	6.3	28
AnBNCz-CN	10	488	3.2	8503	7.0	5.5	3.8	30
	20	492	3.1	10858	9.6	8.6	4.8	31
	30	492	3.2	10590	10.1	9.4	4.9	31
	40	488	3.2	9355	10.5	10.4	4.9	31
AnBNCz-OMe	10	488	3.7	12975	8.1	6.5	4.4	28
	20	492	3.7	7708	9.5	8.3	4.9	29
	30	492	3.8	11913	14.9	14.2	7.6	28
	40	492	3.7	8540	9.4	8.0	4.7	28

[a] Maximum EL wavelength, [b] Turn-on voltage at 1 cd m^{-2}, [c] The luminescence (L), current efficiency (η_c), power efficiency (η_P) and external quantum efficiency (η_{ext}) of the devices at maximum, [d] FWHM of EL spectra.

Table S4. Full-width at half-maximum summary of "hot exciton" based organic light-emitting diodes.[6–18]

Devices	FWHM[a] (nm)	EQE_{max}[b] (%)
PAC：3 wt% BD	42.7	5.3

PAC	59.1	4.5
PPT	80	3.7
PPPT	92	5.9
PAPT	66	7.5
20 wt%:PPT:CBP	58	9.0
20 wt%:PPPT:CBP	72	8.3
20 wt%:PAPT:CBP	53	10.2
IAM	56	6.09
TAM	57	1.46
2-DCPA	58	2.48
3-DCPA	55	2.65
4-DCPA	59	2.07
CBP : 4wt% 2-DCPA	52	2.21
CBP : 4wt% 3-DCPA	50	2.74
CBP : 4wt% 4-DCPA	53	1.74
CBP : 1wt% PloyS-AP	57	3.62
CBP : 5wt% PloyS-AP	58	2.52
BOOAn	80	3.9
2BOOAn	76	5.8
mCP : 16wt% BOOAn	53	6.0
mCP : 16wt% 2BOOAn	49	10.1
PAC	63	10.03
CNNPI	62	2.28
2TriPI-CNNPI	59	2.75
2CzPh-CNNPI	59	5.09
CBP : 5wt% 2CzPh-CNNPI	66	8.42
CBP : 10wt% 2CzPh-CNNPI	72	9.02
PPIDPh	68	10.33
PPIDPhC	66	8.56
PPIDPhO	62	7.90
PITPh	66	6.10
PPITPh	59	11.83
PIAnTp	52	8.36
PyIAnTp	60	8.69
PYTPA	57	4.1
PYTPA-DP	58	6.3
PYTPA-CP	53	5.2
PYTPA-HP	56	9.1
PYTPA-HPC	56	6.5
mCPCN : 1wt% tBOSi	31	3.93
mCPCN : 5wt% tBOSi	32	9.15

mCPCN : 10wt% tBOSi	35	7.41
mCPCN : 15wt% tBOSi	36	6.25
mCPCN : 20wt% tBOSi	38	5.71
PyPO	76	11.1
CBP : 10wt% PyPO	66	7.0

[a] Full-width at half-maximum of EL spectra, [b] External quantum efficiency measured at maximum

References:

1 T. Lu and F. Chen, *J. Comput. Chem.*, 2012, **33**, 580–592.
2 Y. Xu, C. Li, Z. Li, J. Wang, J. Xue, Q. Wang, X. Cai and Y. Wang, *CCS Chem.*, 2022, **4**, 2065–2079.
3 Y. Qu, D. Zhou, F. Kong, Q. Zheng, X. Tang, Y. Zhu, C. Huang, Z. Feng, J. Fan, C. Adachi, L. Liao and Z. Jiang, *Angew. Chem. Int. Ed.*, 2022, **61**, e202201886.
4 R. Wang, D. Hu, L. Xing, Z. Lu, Y. Zhu, Z. Mao, W. Chen, Y. Huo and S. Ji, *Dyes Pigments*, 2023, **215**, 111276.
5 M. Segal, M. Singh, K. Rivoire, S. Difley, T. Van Voorhis and M. A. Baldo, *Nat. Mater.*, 2007, **6**, 374–378.
6 H. Zhang, B. Zhang, Y. Zhang, Z. Xu, H. Wu, P. Yin, Z. Wang, Z. Zhao, D. Ma and B. Z. Tang, *Adv. Funct. Mater.*, 2020, **30**, 2002323.
7 Z. Feng, F. Liu, Z. Cheng, S. Ge, Y. Wang, Z. Yan, X. Ma, Y. Wang and P. Lu, *J. Mater. Chem. C*, 2024, **12**, 3881–3887.
8 W. Wang, J. Bian, K. Chen, C. Li, Y. Long, H. Huang, L. Jiang, J. Zhao, S. Liu, Z. Chi, J. Xu and Y. Zhang, *Angew. Chem. Int. Ed.*, 2024, **63**, e202318782.
9 B. Zhu, T. Sun, S. Guo, H. Zhou, W. Shi, J. Huang, B. Wei, Y. Miao and H. Wang, *Dyes Pigments*, 2023, **215**, 111251.
10 S. Kang, H. Jung, H. Lee, S. Lee, M. Jung, J. Lee, Y. Chul Kim and J. Park, *Dyes Pigments*, 2018, **156**, 369–378.
11 L. Zhang, D. Hu, S. Wang and Y. Ma, *J. Lumin.*, 2024, **273**, 120696.
12 X. Gan, Z. Ding, D. Liu, W. Zheng, B. Ma, H. Zhang, X. Chang, L. Wang, Y. Liu, X. Wu, S. Su and W. Zhu, *Adv. Opt. Mater.*, 2023, **11**, 2300195.
13 Y. Xu, X. Liang, X. Zhou, P. Yuan, J. Zhou, C. Wang, B. Li, D. Hu, X. Qiao, X. Jiang, L. Liu, S. Su, D. Ma and Y. Ma, *Adv. Mater.*, 2019, **31**, 1807388.
14 Z. Cheng, C. Du, S. Ge, Y. Wang, F. Liu, Y. Chang, Y. Lv and P. Lu, *Chem. Eng. J.*, 2023, **474**, 145867.
15 S. Ge, C. Du, Z. Cheng, Y. Wang, Z. Feng, Z. Yan, Y. Hu and P. Lu, *Chem. Eng. J.*, 2024, **489**, 151314.
16 Z. Lu, D. Hu, S.-W. Chen, R. Wang, L. Xing, Y. Zhu, J. Lin, Y. Huo and S. Ji, *J. Mater. Chem. C*, 2024, **12**, 9929–9938.
17 F. Liu, G. Cao, Z. Feng, Z. Cheng, Y. Yan, Y. Xu, Y. Jiang, Y. Chang, Y. Lv and P. Lu, *ACS Appl. Mater. Interfaces*, 2023, **15**, 47307–47316.
18 C. Du, H. Liu, Z. Cheng, S. Zhang, Z. Qu, D. Yang, X. Qiao, Z. Zhao and P. Lu, *Adv. Funct. Mater.*, 2023, **33**, 2304854.